Shaping the future of fuel: Monolithic metal-organic frameworks for high-density gas storage

Bethany M. Connolly,[a,b] David G. Madden,[b] Andrew E. H. Wheatley[a] and David Fairen-Jimenez[b*]*

[a]Department of Chemistry, University of Cambridge, Lensfield Road, Cambridge, CB2 1EW, United Kingdom.

[b]Adsorption & Advanced Materials Laboratory (A^{2}ML), Department of Chemical Engineering & Biotechnology, University of Cambridge, Philippa Fawcett Drive, Cambridge, CB3 0AS, United Kingdom.

[*]e-mails: Andrew E. H. Wheatley, aehw2@cam.ac.uk; David Fairen-Jimenez, df334@cam.ac.uk

Abstract

The environmental benefits of cleaner, gaseous fuels such as natural gas and hydrogen are widely reported. Yet, practical usage of these fuels is inhibited by current gas storage technology. Here, we discuss the wide-ranging potential of gas-fuels to revolutionize the energy sector and introduce the limitations of current storage technology that prevent this transition from taking place. The practical capabilities of adsorptive gas storage using porous, crystalline metal-organic frameworks (MOFs) are examined with regard to recent benchmark results and ultimate storage targets in this field. In particular, the industrial limitations of typically powdered MOFs are discussed while recent breakthroughs in MOF processing are highlighted. We offer our perspective on the future of practical, rather than purely academic, MOF developments in the increasingly critical field of environmental fuel storage.

Background

Despite an explosive report from the Intergovernmental Panel on Climate Change (IPCC) warning of the environmental consequences of increased global warming, current temperatures continue to approach the danger zone of 1.5ºC above preindustrial levels. Correspondingly, widespread environmental damage has already been seen, including vast loss of arctic sea ice, increased frequency of heatwaves and forest fires as well as irreversible animal and plant mass extinctions.[1] The evolution of global surface temperature, based on a range of different data sets, demonstrates both a steady global warming trend since the industrial revolution as well as shockingly rapid warming since the 1970s (**Figure 1**).[2] This environmental impact is widely accepted to correlate with exponentially increased energy consumption since the industrial revolution.[3] Atmosphere-warming greenhouse gasses and other pollutants have traditionally been released by conventional energy generation practices e.g. the burning of non-renewable coal and petrol. With the IPCC report warning that critical changes to energy supply and demand must take place immediately, a complete overhaul

of energy generation and storage practices is essential if future energy demands are to be sustainably realized.

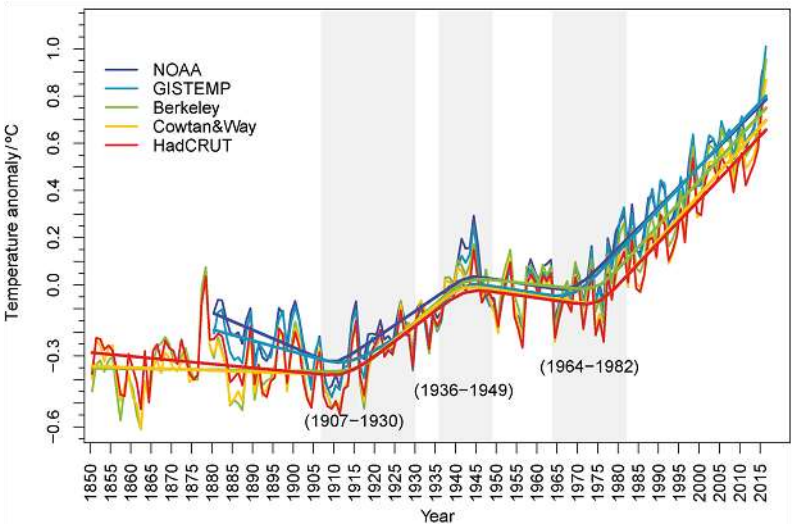

Figure 1. Changepoint analysis of global temperature (combined land and ocean) trends (1850 – 2015) for data sets collected by NOAA (The National Oceanic and Atmospheric Administration), GISTEMP (Goddard's Global Surface Temperature Analysis collected by The National Aeronautics and Space Administration), Berkeley (Berkeley Earth Surface Temperature), HadCRUT (The Hadley Centre Climate Research Unit) and Cowtan&Way (Revised HadCRUT data). Reproduced from **Reference 2** with permission of IOP publishing.

One of the best solutions to mitigate global warming is the use of cleaner gaseous fuels. With abundant natural reserves and reduced greenhouse gas emissions relative to solid coal and liquid petroleum, the usage of natural gas (NG, primarily composed of methane) is predicted to increase significantly.[4] Among the potential uses of gaseous fuels, a much sought-after application is in automobile engines. Considering only the European market, the addition of *ca.* 3 million cars each year increases annual energy consumption by 4%.[5] Since NG combustion engines emit 70, 87 and 20% less CO, NO_x and CO_2, respectively, than gasoline combustion engines, this would bring a staggering reduction in global emissions, as well as a much-needed improvement in local air quality in highly populated areas.[5] An even more promising energy vector is clean, gaseous hydrogen. With ongoing development of affordable and environmentally friendly production methods,[6] as well as an outstanding gravimetric energy density of 120 MJ kg–1 compared to 47.2 MJ kg–1 for gasoline, widespread utilisation of this potentially zero-carbon emission gas, would revolutionize the energy industry and lessen current oil dependence in what is termed 'The Future Hydrogen Economy'.[7] Fuel cell vehicles (FCV), which environmentally convert hydrogen to electricity, offer further benefits over not just traditional internal combustion engines but also popular battery-powered vehicles, including substantial enhancements in driving range, with distances exceeding 500 km proposed.[8]

In spite of the potential benefits, the limitations of current gas storage technology remain a significant barrier to widespread gas-fuel usage. Obviously, the required technology differs

drastically from that which underpins the storage of traditional solid and liquid-based fossil fuels. From a practical perspective, gas-fuel must be densely stored for feasible onboard usage. Taking NG as an example, compressed natural gas (CNG) is stored traditionally at room temperature under high pressures (*ca.* 180 – 250 bar) in robust, thick-walled steel tanks. The low storage capacity of these tanks, coupled with the high mass of the storage vessels, which contribute at least 90% to the total system mass,[9] and the cost of complex, multi-stage compressors prevent translation of this technology to NG powered vehicles. The main consequence is that both the driving range and vehicle payload capacity are significantly limited. Additionally, the onboard storage of highly pressurized flammable-gas tanks presents obvious safety concerns. Low-pressure storage of liquified natural gas (LNG) may provide fuel with up to 2.4 times higher energy density than CNG at 250 bar. Still, the liquification of NG demands energy-intensive cooling to less than 110 K as well as bulky/heavy insulative chambers to maintain cryogenic temperatures, mostly limiting this process to applications in transoceanic shipping.[10]

To stimulate the development of new technologies that would increase NG viability by reducing the practical, safety and economic barriers to its distribution and usage, the U.S. Department of Energy (DOE) set an ambitious volumetric storage target for NG of 263 cm^3 (STP) cm^{-3} at 65 bar and 298 K.[11] This is identical to the volumetric capacity of CNG at 250 bar and 298 K.[12] Subsequently, the Advanced Research Projects Agency-Energy (ARPA-E) set the methane deliverable capacity between 65 and 5.8 bar to 315 cm^3 (STP) cm^{-3}, a target that is often considered too high to be reached.[13] In any case, recommended pressures of *ca.* 65 bar and even 100 bar are highly practical, being cost-effectively achieved using relatively inexpensive compressors and requiring lighter storage tanks.[5] This offers not only safety benefits but also improvements in large-scale industrial economics.

In addition to NG, the DOE has collaborated with both the U.S. Council for Automotive Research and a number of U.S. energy companies to establish additional targets for on-board hydrogen storage in light-duty vehicles. The ultimate aim is to develop a complete technology (i.e. materials, tank, H_2 delivery system, etc.) that can compete with incumbent vehicle technology by achieving a comparable 300 – 500 mile driving range while simultaneously meeting cost and safety requirements. These ultimate H_2 storage targets are highly ambitious, standing at 6.5 wt.% and 50 g L^{-1}; crucially, these cannot be achieved by compression.[14] Moreover, while this DOE target appears ambitious, the ultimate H_2 storage requirements will, in fact, need to be significantly higher to account for the additional weight of the complete H_2 storage *and* delivery system. State-of-the-art commercial FCVs produced by companies such as Toyota rely on ambient temperature H_2 storage at a mammoth 700 bar.[15] Yet even under such immense compression, the maximum H_2 storage density stands at only 40

g L^{-1}. Moreover, in order to meet current FCV operating specifications, the fuel *delivery* (i.e. release) pressure and temperature must range between 5 – 12 bar and 233 – 358 K, respectively, though the *storage* temperature/pressure conditions may fall significantly outside this range. These guidelines for on-board H_2 storage identify 160 and 430 bar as 'low' and 'moderate' storage pressures, respectively. Obviously, H_2 storage systems which rely on excessively high pressures and/or low temperatures are costly, impractical and energy consuming to achieve and maintain. Neither of these gas-fuel targets (CH_4 or H_2) can be achieved by traditional high-pressure compression or low temperature liquification.[7]

Adsorbed hydrogen and Natural Gas

A range of alternative storage techniques for gas-fuels have been proposed, with chemical storage of H_2 as metal-hydrides being of particular note.[16] Though promising results have been achieved via this process (e.g. inexpensive MgH_2 has a 7.6 wt.% H_2 capacity),[17] an inherent pitfall of this technology is the highly exothermic nature of metal hydride formation and subsequently endothermic hydrogen fuel regeneration. Heat transfer to, and from, the metal hydride reactor bed, as well as slow dehydrogenation kinetics, are significant challenges in chemisorption.[18] Alternatively, physisorbed NG (ANG) and H_2, in which the adsorbate is stored in the internal porosity of an adsorbent material, are regarded as a highly efficient means of achieving high-density gas storage.[12,19] Weak physisorption-based storage offers numerous practical advantages over energy-intensive metal hydride formation, including fast adsorption/desorption kinetics and high cyclability.[20]

The strength of the gas-adsorbent interaction in porous materials is dependent on both the size and chemical properties of the adsorbate (e.g. polarity) as well as pore shape/diameter (*d*) and surface chemistry of the adsorbent.[21,22] The origin of the adsorption comes from the short-range Paulie repulsion as well as attractive forces such as van der Waals. On top of these, electrostatic interactions play a crucial role, especially when the adsorbent expresses functional groups and the adsorbates present a dipolar or a quadrupolar moment.[23] For an infinitely wide pore, i.e. an open surface, a gas molecule only experiences the attractive potential energy of the wall where it is adsorbed. As pore-diameter decreases, the potential fields of opposing pore walls overlap to create an enhanced energy well in the middle (**Figure 2a**).[24,25] This enhancement in negative potential energy is manifested significantly for pore diameters below 2 nm, i.e. microporous materials. A minimum practical pore diameter obviously exists, below which the molecules cannot fit, the kinetics of adsorption are too slow or the number of molecules that can be adsorbed is reduced. These effects lead to gas physisorption in microporous materials being considered to be energetically preferred to that in meso- (pore sizes between 2 and 50 nm) or macroporous (pore sizes larger than 50 nm) materials, due to the balance of high accessible internal surface area and enhanced gas adsorption properties.[5]

It's appeal notwithstanding, gaseous fuel adsorption by purely microporous materials presents practical problems of fuel accessibility. Due to the above-discussed dependence of adsorbent interaction on pore diameter, gaseous species are adsorbed by materials with a narrow pore-size distribution over a narrow pressure range. Due to their strong interaction potential with narrow micropores, gases rapidly saturate purely microporous materials at low pressure. This is described by a Type I adsorption isotherm (**Figure 2b**). Since there typically exists a minimum working pressure below which stored fuel cannot be practically accessed (*ca.* 5 bar for vehicular H_2 and CH_4 storage),[26,27] the energetically favorable adsorption of gases at low pressure means that the accessible adsorbed gas (i.e. the *working capacity*) is significantly lower than the total amount stored. In contrast, materials with wide pore-size distributions (i.e. mixed micro-/meso-/macroporous materials) offer varying interaction potentials, adsorb over a wider range of pressures and hence have much higher working capacities, as illustrated by a combined Type I and IV isotherm (**Figure 2c**). It is therefore clear that, if gas fuel storage by physisorption is to be practically realized, then precise control over the adsorbant material's porosity is vital.

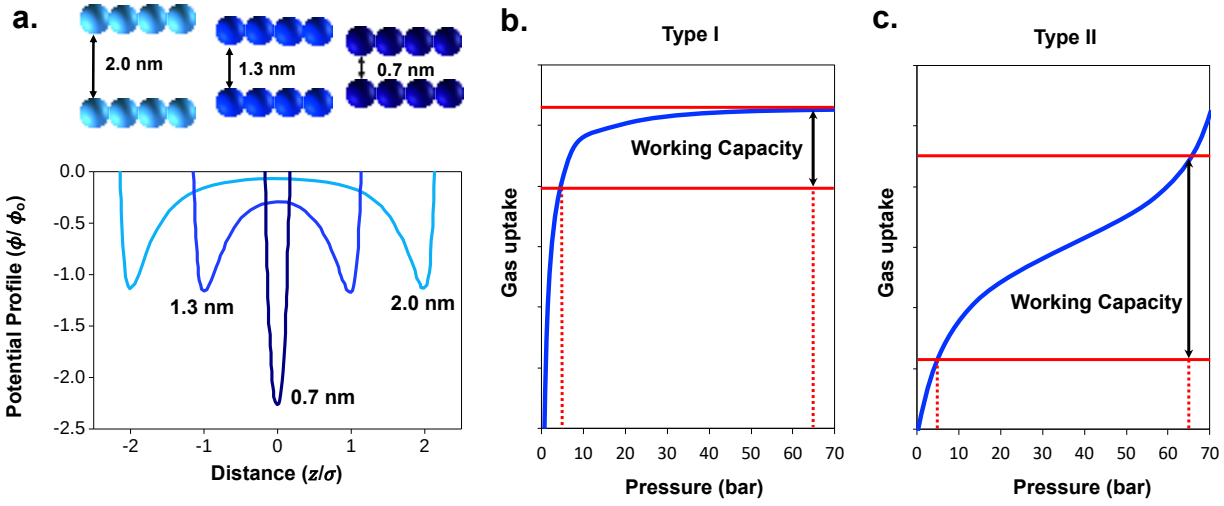

Figure 2. a. Comparison of potential energy profiles ($\phi/\ \phi_o$), approximated from the Steel potential energy function, for a gas molecule (CH_4, kinetic diameter, $\sigma = 0.38$ nm) a distance (z) from the centre of model graphitic micropores with diameters 2.0 nm (sky blue), 1.3 nm (royal blue) and 0.7 nm (navy blue) Data digitized from **Reference 22**. **b.** Type I isotherm for an adsorbent with a narrow pore-size distribution i.e. purely microporous. **c.** Type I + IV isotherm for an adsorbent with a wide pore-size distribution i.e. mixed micro-/mesoporous.

Gas storage in metal-organic frameworks

Amongst known porous materials, metal-organic frameworks (MOFs) stand out as a safe, low energy means of dense gas-fuel storage. MOFs are a diverse family of high porosity, coordination polymers that result from the crystalline self-assembly of metal ions/metal oxide clusters[28,29,30] with multi-dentate organic linkers.[31] The modular nature of these materials allows high synthetic tuneability,

with over 90,000 distinct structures having been added to the Cambridge Structural Database (CSD).[32] Significantly, the compositional and structural variations between these materials allow comprehensive control over their chemical and physical properties. For example, the choice of metal and its degree of saturation influences both the thermal/chemical stability as well as structural topology and thus porosity of the framework. The inherent porosity of crystalline MOFs corresponds with high surface areas, typically above 1000 m^2 g^{-1}. In 2018, and starting from a computational design of the structure, Kaskel developed DUT-60, a material with a record-setting BET area of 7800 m^2 g^{-1} (**Figure 3**).[33] MOFs with large pore volumes facilitate high gas uptake,[34] although this can also present critical challenges related to the materials having low densities, as described below.

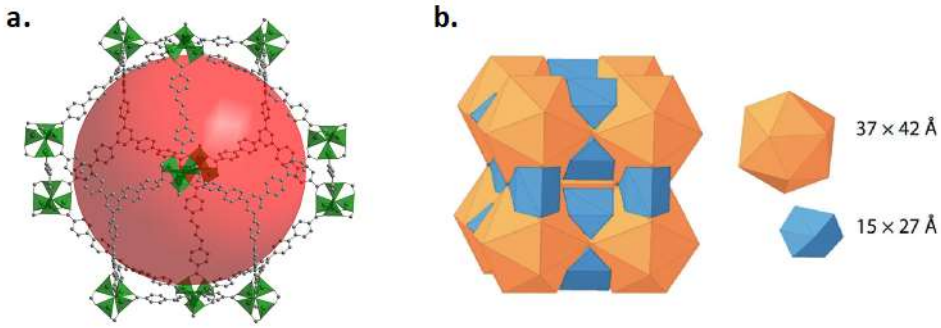

Figure 3. a. DUT-60 framework structure showing the arrangement of 1,3,5-tris(4′-carboxy[1,1′-biphenyl]-4-yl)benzene and 1,4-bis-*p*-carboxyphenylbuta-1,3-diene linkers (grey) with $Zn_4O(CO_2)_6$ clusters (green polyhedra). Pore volume is indicated by the space-filling sphere (red). **b.** Spatial arrangement and dimensions of the mesopore system (orange and blue polyhedra) within DUT-60. Reproduced from **Reference 33** with permission of John Wiley and Sons Inc.

The trailblazing work on 3D coordination polymers was first published by Saito and co-workers in 1959.[35] Following the work of Robson and Werner in the design of 3D coordination polymers,[36,37] Yaghi[38,39] and Kitagawa[40] pioneered the use of MOFs and PCPs in gas adsorption applications. Since then, significant synthetic advancements have been made, resulting in the tailoring of MOF structures for maximized gravimetric gas storage capacity (i.e. cm^3 (STP) g^{-1} – per unit of mass). Significantly, a benchmark computational and experimental study of a diverse series of MOFs was recently used to demonstrate the linear relationship between pore volume and H_2 gravimetric capacity.[14] This study showed that, when allowing flexibility in the temperature range dictated by the U.S. DOE, Cu-based NU-125 was found to achieve a record *gravimetric* H_2 storage, with a working capacity of 8.5 wt.% when operating under temperature-pressure swing conditions (77 K and 100 bar at adsorption, and 160 K and 5 bar at desorption). The *volumetric* working capacity of NU-125 in these conditions was calculated to be 49 g L^{-1} assuming maximum crystal density i.e. ideal packing of the defect-free material.

Based on the outstanding gravimetric capacities of numerous MOFs, such as NU-125, for the storage of gaseous fuels, it is evident that they have the potential for wide-reaching environmental

impact in the energy sector. Yet, significant barriers to widespread industrial MOF usage remain. In addition to the gravimetric gas storage capacity described above, volumetric (e.g. cm^3 (STP) cm^{-3}) capacity – which determines the volume of gas which can be stored as a function of the volume of an adsorbent-filled tank – is a critical measure of industrial viability in gas storage. If gravimetric capacity is low, the payload capacity of the tank is diminished. This reduces fuel economy via the energy-consuming transportation of the heavy on-board tank. If volumetric capacity is low, excessively voluminous tanks are required to store the quantity of fuel required for feasible transport; a similar problem is faced in industrial adsorption-based separation columns.[41] While substantial progress in the synthesis of MOFs with high *gravimetric* capacities for CH_4, H_2 and other gases has been made, research directed towards achieving practical *volumetric* capacities has been somewhat overlooked. High gravimetric capacities are achieved in porous materials by maximizing void fractions, yet this yields low-density frameworks. However, volumetric capacity is maximized by balancing void fraction with high crystal density. This relationship was computationally studied by Snurr and co-workers, who performed high throughput computational screening of 18,383 MOFs for H_2 storage capacity.[42] Maximum gravimetric capacity was achieved in materials with void fractions exceeding 0.9, while volumetric capacity was maximized at a void fraction of ca. 0.75. The contrasting topological requirements of these two physical properties represent an inherent limitation to the development of porous materials for feasible large-scale gas storage.

A significant issue with many reports of state-of-the-art gas storage MOFs is that their capacities are recorded gravimetrically and converted to volumetric capacity using the theoretical single-crystal density of the adsorbing MOF. Traditionally, however, MOFs have been synthesized as micro- or nanoscale crystals, with the resulting bulk material being a loosely packed, fine powder.[20] It follows that volumetric capacities calculated from single crystal density *do not take into consideration* the low packing efficiency of individual MOF crystals. This has been reported to lead to the overcalculation of practical volumetric gas storage capacity by as much as 300%.[43] This overcalculation stems from the inevitable complexity of measuring bulk densities in fine powders. From a practical perspective, even if a MOF with both high gravimetric and theoretical volumetric gas storage capacity is synthesized, a non-optimized, powdered material will be incapable of reaching that volumetric gas storage potential. To achieve the wide-ranging potential of MOFs in gas storage, powders must be processed into more practical materials.

Industrially viable adsorption

With the arrival of MOFs to the market,[44] an extensive range of MOF-shaping techniques have been reported,[45] including 3D printing,[46,47] foaming,[48] chemical vapor deposition (CVD) onto thin films[49] and use of supports such as cordierite[50,51] or activated carbons.[52] Yet, the resulting low-density

products often perform less well than predicted, demonstrating the importance of combining high adsorbent density and mechanical robustness during shaping. Meeting this target would have a number of critical benefits. These include eliminating pressure drops due to powder compaction and the accompanying resistance to gas flow, minimization of dusting and materials loss, and the avoidance of pore collapse or blockage upon the application of high-pelletization pressures.

Attempts to pelletise MOFs have generally focussed on two approaches. The first involves powder compaction by the application of pressure (typically 10 to 100 MPa).[53] The aim of this process is to achieve a bulk density that approaches the MOFs single-crystal density by minimizing interparticle space. Denser pellets of a range of MOFs have been reported using this approach. Farrusseng and co-workers recorded a positive linear relationship between applied pressure and mechanical strength for a range of densified MOF pellets of Cu- and Zr-MOFs.[54] Despite achieving 1.8 – 3.4 fold increases in MOF bulk density compared to the corresponding powders, this synthetic approach caused substantial losses of BET area due to pore collapse. For example, exposure of UiO-66-NH_2 [$Zr_6O_4(OH)_4$(2-amino-1,4-benzenedicarboxylate)$_6$] to 63 – 82 MPa applied pressure resulted in a *ca.* 80% loss of BET area. This is the result of pressure-induced amorphization via the cleavage of chemical bonds in the MOF, an inherent consequence of applying mechanical force.[55]

In a similar vein, HKUST-1 [Cu_3(1,3,5-benzenetricarboxylate)$_2$], was computationally identified by Peng et al. to exceed DOE targets for methane storage, with a volumetric capacity of 270 cm^3 (STP) cm^3 (65 bar) expected. Experimentally, however, the powder density of HKUST-1 (0.43 g cm^{-3}) was so much lower than the single crystal density (0.883 g cm^{-3}) that the volumetric capacity measured for the powder was less than 50% of the theoretical value. Moreover, while the application of high pressures (4.54 tonnes) achieved high density (1.104 g cm^{-3}) pelletized disks, the low mechanical stability of these otherwise promising MOF pellets resulted in a 59% loss of pore volume and, correspondingly, no significant increase in volumetric storage capacity was observed.[34] Zhou and co-workers studied the impact of extrusion pressure on the physical properties of highly stable PCN-250, which is comprised of $Fe_3(\mu_3\text{-}O)$ oxoclusters coordinated by 3,3′,5,5′-azobenzenetetracarboxylate linkers. The application of asymmetric pressure during extrusion was found to incur irreversible phase transformations despite the retention of crystallinity. The resulting PCN-250 analogs (PCN-250′ and PCN-250″) displayed isomerically flipped N=N bonds in some of the tetratopic linkers. In particular, PCN-250″ showed both reduced unit-cell volume (–1.33 %) and gravimetric CH_4 uptake (–21.4 %).[56] To help with the prediction of properties of pelletized materials, we recently developed an interactive map of the structure-mechanical landscape of MOFs by performing a multi-level computational analysis on 3,385 MOFs.[57] Using artificial neural networks, we were able to reveal the sensitivity of structural parameters such as network topology and porous

texture to pressure, allowing us to predict the performance of existing and future MOFs through a readily available machine learning algorithm.

The second approach to attempting to achieve free-standing, industrially viable MOF pellets avoids high pressures and instead involves the addition of chemical binders e.g. typically long-chain polymers such as polyvinylpyrrolidone (PVP) and poly (*N*-methylolacrylamide) (PNMA).[58,59] These binders act as adhesives, adhering individual MOF crystals in e.g. extrusion,[60] emulsion templating[61] and granulation[62] processes. Despite high resulting mechanical strength, which increases ease of usage from a practical perspective, materials obtained in this way must contain a significant percentage of binder, both introducing new chemical functionality and preventing MOF density from being maximized. Denayer and co-workers produced sub-millimeter MIL-53 [Al(OH)(O_2C-C_6H_4-CO_2)] pellets comprising 13 wt.% polyvinyl alcohol (PVA).[63] Besides the increased synthetic complexity and cost of producing such composite materials, binders reduce gas uptake capacity by decreasing the total bulk quantity of MOF in each pellet without achieving substantial gains in total packing efficiency/density. Chang et al. reported the macroscopic granulation processing of Fe-, Zr- and Cr-based MOFs using 5 wt.% amorphous-phase mesoporous ρ-alumina as binder.[64] Even though the application of relatively moderate binder quantities, bulk densities of the obtained materials were significantly lower than the theoretical crystal densities of the studied MOFs (i.e. 0.67 g cm^{-3} vs. 1.20 g cm^{-3} for UiO-66). Additionally, bulky binder molecules can further block pores, reducing accessible porosity and preventing efficient gas sieving.[65] Overall, observed losses of crystallinity and accessible porosity by the two traditional processing methods outlined here have, to date, resulted in non-optimized MOF products that cannot approach their maximum potential for gas-based applications.

Ideally, the future of MOFs for gas-fuel applications lies in the non-trivial densification of *pure* materials without loss of accessible porosity.[62] We recently reported a novel, room-temperature sol-gel synthesis of robust, centimeter-scale monolithic advanced MOF, $_{mono}$ZIF-8 [Zn(2-methylimidazolate)$_2$], without the use of chemical binders or applied pressures.[43] The resulting transparent, glassy-looking, crystalline material displayed high bulk mechanical strength (hardness, *H*, = 0.43 ± 0.03 GPa) and BET area (S_{BET} = 1423 m^2 g^{-1}) and a density that, at ρ_b = 1.05 g cm^{-3}, compares closely to that of the corresponding theoretical single crystal (ρ_b = 0.95 g cm^{-3}). Excitingly, the generality of this novel synthesis has been demonstrated through its extension to other MOFs, starting with HKUST-1 (**Figure 4a**).[66] The remarkable physical and mechanical properties displayed by $_{mono}$HKUST-1 (ρ_b = 1.06 g cm^{-3}, S_{BET} = 1288 m^2 g^{-1} and *H* = 0.46 ± 0.03 GPa) (**Figure 4b**) resulted in an outstanding volumetric methane uptake capacity of 261 cm^3 (STP) cm^{-3} (65 bar, 298 K). Not only does this substantially exceed the previously reported results for HKUST-1 compacted under a range of pressures,[34] but it renders the first densified material to effectively reach the DOE

target for methane storage.[12] Furthermore, comparable sol-gels of HKUST-1 (comprising only the MOF and ethanol) have recently demonstrated further applicability towards alternative shaping processes, including 3D printing.[67]

Figure 4. a. Crystal structure of HKUST-1, **b.** Optical image of *mono*HKUST-1, **c.** Crystal structure of UiO-66, **d.** Optical image of *mono*UiO-66, **e.** Comparison of absolute CH_4 uptake in *mono*HKUST-1 (white star), *mono*UiO-66 (green circle) and simulated UiO-66 (white square) between 0 – 100 bar at 298 K. Dashed red line indicates the DOE target for CH_4 storage in a densified material at 65 bar (298 K), **f.** Table showing both the total absolute CH_4 uptake and working capacity in each MOF at 5, 65 and 100 bar. Working capacity is calculated from the uptake at the maximum storage pressure (65 or 100 bar) minus the uptake at the minimum desorption pressure (5 bar).

While the development of the densified Cu-based MOF *mono*HKUST-1, with its record-setting volumetric methane storage, represents a significant breakthrough in the field of powder shaping, it still does not yield an industrially optimized material.[66] The presence of open Cu(II) sites in this MOF's coordinatively unsaturated di-copper paddle-wheel-based structure results in a high water affinity. A gradual and irreversible loss of crystal structure through exposure to humidity is observed e.g. under ambient conditions and in the presence of NG.[68] If MOFs are to be practically applied to gas storage applications, it is clear that the process of synthesizing dense and porous monolithic materials must be extended to a wider range of materials with a host of precisely tuneable properties e.g. air/water stability, mechanical strength *and* variable pore size and functionalities.

Enhanced chemical stability is often observed in MOFs containing high oxidation state metals since these can form strong metal-linker bonds. Zirconium MOFs are the prototypical example of this; the Zr(IV) centers exhibit hard-hard coordination to carboxylate linkers to achieve chemically, mechanically and thermally stable frameworks.[69] Through a gel-based synthesis, different groups

have extended the possibility of creating monolithic MOFs to the archetypical zirconium-MOF UiO-66 [$Zr_6O_4(OH)_4$(benzene-1,4-dicarboxylate)]. Although the first attempts resulted in mm-sized structures (**Figure 5a – c**),[70] Horcajada and co-workers were able to create cm-sized xero- and aero-gels with hierarchical porosity (**Figure 5d – f**).[71] Very recently, Nakanishi et al. described controlled trimodal structures, that is, with micro-, meso- and macro-porosities, of UiO-66-NH_2 (**Figure 5g – i**).[72] However, due to the large mesopore volumes, all these monoliths returned low densities (*ca.* 0.39 g cm^{-3}). In contrast, by synthetically varying the drying conditions employed at the end of the synthesis (e.g. the boiling point of washing solvent and drying temperature), we have been able to demonstrate that the bulk physical properties of a monolithic MOF can be tuned with a high level of experimental control. For example, we have been able to produce robust $_{mono}$UiO-66 (**Figure 4d**) and $_{mono}$UiO-66-NH_2 samples with bulk densities varying between 0.43 – 1.05 g cm^{-3}, while single-crystal UiO-66 exhibits a density of 1.20 g cm^{-3}. This density variation was achieved by the novel, controlled inclusion of mesoporosity within the macrostructure of the otherwise purely microporous MOF.

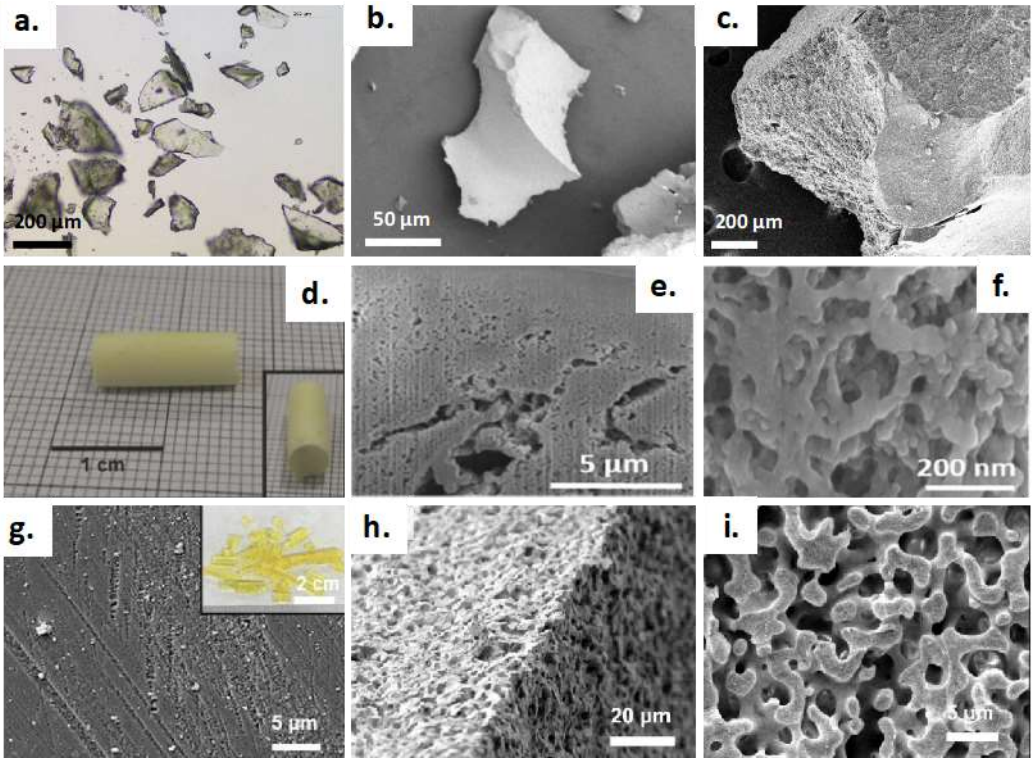

Figure 5. a. Optical and **b – c.** SEM images of UiO-66 monolithic xerogels. Reproduced from **Reference 70** with permission from the Royal Society of Chemistry. **d.** Optical and **e – f.** SEM images of UiO-66-NH_2 aero-monolith obtained by supercritical CO_2 drying of a MOF gel. Reproduced from **Reference 71** with permission from the Royal Society of Chemistry. **g – i.** SEM images of dried UiO-66-NH_2 gel. Inset in **g.** Optical image of a monolith. Reproduced with permission from **Reference 72** with permission of John Wiley and Sons Inc.

As already discussed, in addition to total gas uptake, another parameter of critical importance is the working capacity of an adsorbent. That is, the *usable* volume of adsorbed gas achievable under practical working conditions. MOFs that are ordinarily purely microporous, such as UiO-66 and

HKUST-1, typically demonstrate high gas uptake at low pressure followed by pore saturation i.e. Type I adsorption isotherms (**Figure 2b**). The result of this is a high *total* gas uptake but low *working capacity*. By synthetically including variable volumes of mesoporosity into the macrostructure of normally purely microporous UiO-66, it proved possible to beneficially convert the Type I isotherm shape normally associated with this MOF to Type I + IV isotherm (**Figure 4e**). This transition was a consequence of the controlled introduction of delayed gas condensation in the wider mesoporous cavities at higher pressures. This structural modification and its resultant alteration to the absorptive properties of the MOF yielded outstanding improvements in the working capacity of *mono*UiO-66 (up to 261 cm^3 (STP) cm^{-3}, 5 – 100 bar, 298 K) compared to that of the theoretical, purely microporous material (139 cm^3 (STP) cm^{-3}) or to experimental, purely microporous *mono*HKUST-1 (235 cm^3 (STP) cm^{-3}) (**Figure 4e,f**). Hence, not only can air-stable, high-density monolithic MOFs now be synthesized with retention of accessible porosity, but we have further demonstrated that unprecedented levels of synthetic control can be exerted on the materials to enhance the gas adsorption capacity beyond theoretical maxima in purely microporous and defect-free materials.

Outlook

In the field of environmental preservation and remediation, numerous MOFs exhibiting significant potential have been reported.[73] The high modularity of these unique materials allows for precise tuning of both chemical and physical properties, making them applicable to all stages of environmental energy usage.[74] Outstanding results have been reported not only in the high-density storage of environmental gas-fuels (including NG and hydrogen) but also in molecular sieving for gas stream purification and the capture of environmental pollutants.[75] Despite these significant achievements, the full potential of MOFs is far from being achieved and their industrial usage remains limited to just a few examples e.g. BASF have recently tested the viability of a NG-powered vehicle fleet.[76] Such poor progress stems not only from the current cost barriers to mass production,[77] but also from a technical inability to process the obtained adsorbents into *practically* viable materials. While some materials have been shown to be capable of being produced using economically more feasible synthesis routes such as aqueous and liquid assisted grinding (LAG) methods,[77] the vast majority of MOFs still require energy-intensive solvothermal synthesis, after which bulk powders need to be processed into usable shaped bodies. These approaches have thus far failed to produce viable high-density materials that can achieve the challenging targets set by the DOE for NG and H_2 storage and as such newer synthetic methods will be required to produce next-generation MOFs. On top of that, and in particular for NG and H_2 storage, another critical barrier that remains is the need to develop a MOF that, even with a crystallographic density, can meet these DOE targets.

More than 90,000 unique MOFs have been structurally characterized to date,[32] each with diverse and distinct chemical and physical properties. This raises the question, how do we choose the ideal material for a target application? In this respect, the considered combination of computational and experimental chemistry will likely yield the most promising results.[78] Being crystalline materials, MOFs can be easily engineered through *ad hoc* building blocks, where the organic ligands enrich the surface chemistry and the metal nodes define the geometry.[79] With this in hand, recent advances in data mining and computational simulation of known MOF structures have already provided unrivaled insights into the design and selection of materials for specific applications.[80] We and others have used high-throughput simulations to develop extensive and dynamic structure-property relationships, being able to report a full cycle of novel material development for diverse applications, including the storage of H_2 and NG as well as other molecules.[81] This demonstrates not only the unrivaled potential of MOFs to revolutionize environmental gas capture and storage but further highlights the significance of fully utilizing computational chemistry to both rationalize and unlock their potential.[82]

Acknowledgments

This project has received funding from the European Research Council (ERC) under the European Union's Horizon 2020 research and innovation programme (NanoMOFdeli), ERC-2016-COG 726380 and from Innovate UK (project reference, 104384). D.F.-J. thanks the Royal Society for funding through a University Research Fellowship. B.M.C. thanks the Ernest Oppenheimer Fund (Cambridge).

References

(1) Allen, M.; Dube, P. O.; Solecki, W.; Aragón-Durand, F.; Cramer, W.; Humphreys, S.; Kinuma, M.; Kala, J.; Mahowald, N.; Mulugetta, Y.; et al. *IPCC Special Report: Global Warming of 1.5°C*; 2018.

(2) Rahmstorf, S.; Foster, G.; Cahill, N. Global Temperature Evolution: Recent Trends and Some Pitfalls. *Environ. Res. Lett.* **2017**, *12* (5). https://doi.org/10.1016/j.micromeso.2011.10.045.

(3) Ummenhofer, C. C.; Meehl, G. A. Extreme Weather and Climate Events With Ecological Relevance: A Review. *Phil. Trans. R. Soc. B.* **2017**, *372* (1723), 1–13. https://doi.org/10.1098/rstb.2016.0135.

(4) *BP Energy Outlook, BP p.l.C.*; 2018.

(5) Kumar, K. V.; Preuss, K.; Titirici, M. M.; Rodríguez-Reinoso, F. Nanoporous Materials for the Onboard Storage of Natural Gas. *Chem. Rev.* **2017**, *117* (3), 1796–1825. https://doi.org/10.1021/acs.chemrev.6b00505.

(6) Dincer, I.; Acar, C. Innovation in Hydrogen Production. *Int. J. Hydrogen Energy* **2017**, *42* (22), 14843–14864. https://doi.org/10.1016/j.ijhydene.2017.04.107.

(7) Berenguer-Murcia, Á.; Marco-Lozar, J. P.; Cazorla-Amorós, D. Hydrogen Storage in Porous Materials: Status, Milestones, and Challenges. *Chem. Rec.* **2018**, *18* (7), 900–912. https://doi.org/10.1002/tcr.201700067.

(8) Álvarez Fernández, R.; Corbera Caraballo, S.; Beltrán Cilleruelo, F.; Lozano, J. A. Fuel Optimization Strategy for Hydrogen Fuel Cell Range Extender Vehicles Applying Genetic Algorithms. *Renew. Sustain. Energy Rev.* **2018**, *81*, 655–668. https://doi.org/10.1016/j.rser.2017.08.047.

(9) Rowsell, J. L. C.; Yaghi, O. M. Strategies for Hydrogen Storage in Metal-Organic Frameworks. *Angew. Chem. Int. Ed.* **2005**, *44* (30), 4670–4679. https://doi.org/10.1002/anie.200462786.

(10) Deniz, C.; Zincir, B. Environmental and Economical Assessment of Alternative Marine Fuels. *J. Clean. Prod.* **2016**, *113*, 438–449. https://doi.org/10.1016/j.jclepro.2015.11.089.

(11) ARPA-E. DE-FOA-0000672: Methane opportunities for vehicular energy https://arpa-e-foa.energy.gov/Default.aspx?Search=DE-FOA-0000672 (accessed Oct 10, 2019).

(12) Gallagher, J. Towards Methane Targets. *Nat. Energy*. Springer US 2018, p 86. https://doi.org/10.1038/s41560-018-0100-9.

(13) Simon, C. M.; Kim, J.; Gomez-Gualdron, D. A.; Camp, J. S.; Chung, Y. G.; Martin, R. L.; Mercado, R.; Deem, M. W.; Gunter, D.; Haranczyk, M.; et al. The Materials Genome in Action: Identifying the Performance Limits for Methane Storage. *Energy Environ. Sci.* **2015**, *8* (4), 1190–1199. https://doi.org/10.1039/c4ee03515a.

(14) García-Holley, P.; Schweitzer, B.; Islamoglu, T.; Liu, Y.; Lin, L.; Rodriguez, S.; Weston, M. H.; Hupp, J. T.; Gómez-Gualdrón, D. A.; Yildirim, T.; et al. Benchmark Study of Hydrogen Storage in Metal-Organic Frameworks under Temperature and Pressure Swing Conditions. *ACS Energy Lett.* **2018**, *3* (3), 748–754. https://doi.org/10.1021/acsenergylett.8b00154.

(15) Toyota Mirai Brochure, 2019.

(16) Barthelemy, H.; Weber, M.; Barbier, F. Hydrogen Storage: Recent Improvements and Industrial Perspectives. *Int. J. Hydrogen Energy* **2017**, *42* (11), 7254–7262. https://doi.org/10.1016/j.ijhydene.2016.03.178.

(17) Zhang, X.; Leng, Z.; Gao, M.; Hu, J.; Du, F.; Yao, J.; Pan, H. Enhanced Hydrogen Storage Properties of MgH2 Catalyzed With Carbon-Supported Nanocrystalline TiO2. *J. Power Sources* **2018**, *398* (June), 183–192. https://doi.org/10.1016/j.jpowsour.2018.07.072.

(18) Afzal, M.; Mane, R.; Sharma, P. Heat Transfer Techniques in Metal Hydride Hydrogen Storage: A Review. *Int. J. Hydrogen Energy* **2017**, *42* (52), 30661–30682. https://doi.org/10.1016/j.ijhydene.2017.10.166.

(19) Allendorf, M. D.; Hulvey, Z.; Gennett, T.; Ahmed, A.; Autrey, T.; Camp, J.; Seon Cho, E.; Furukawa, H.; Haranczyk, M.; Head-Gordon, M.; et al. An Assessment of Strategies for the Development of Solid-State Adsorbents for Vehicular Hydrogen Storage. *Energy Environ. Sci.* **2018**, *11* (10), 2784–2812. https://doi.org/10.1039/C8EE01085D.

(20) Wu, B.; Ma, H.; Pan, Z.; Wang, J.; Qu, W.; Wang, B. Review on Processing of Metal–Organic Framework (MOF) Materials Towards System Integration for Hydrogen Storage. *Int. J. Energy Res.* **2015**, *39*, 607–620.

(21) Cychosz, K. A.; Thommes, M. Progress in the Physisorption Characterization of Nanoporous Gas Storage Materials. *Engineering* **2018**, *4* (4), 559–566. https://doi.org/10.1016/j.eng.2018.06.001.

(22) Wu, K.; Chen, Z.; Li, X.; Dong, X. Methane Storage in Nanoporous Material at Supercritical Temperature Over A Wide Range Of Pressures. *Sci. Rep.* **2016**, *6*, 1–10.

(23) Sullivan, D. E. Van Der Waals Model of Adsorption. *Phys. Rev. B* **1979**, *20* (10), 3991–4000. https://doi.org/10.1103/PhysRevB.20.3991.

(24) Cui, X.; Bustin, R. M.; Dipple, G. Selective Transport of CO2, CH4, and N2 in Coals: Insights From Modeling of Experimental Gas Adsorption Data. *Fuel* **2004**, *83* (3), 293–303. https://doi.org/10.1016/j.fuel.2003.09.001.

(25) Saha, D.; Grappe, H. A.; Chakraborty, A.; Orkoulas, G. Postextraction Separation , On-Board Storage, and Catalytic Conversion of Methane in Natural Gas: A Review. *Chem. Rev.* **2016**, *116*, 11436–11499.

(26) ARPA-E. MOVE Program Overview https://arpa-e.energy.gov/sites/default/files/documents/files/MOVE_ProgramOverview.pdf (accessed Feb 20, 2020).

(27) DOE. DOE Technical Targets for Onboard Hydrogen Storage for Light-Duty Vehicles https://www.energy.gov/eere/fuelcells/doe-technical-targets-onboard-hydrogen-storage-light-duty-vehicles (accessed Feb 20, 2020).

(28) Tsivion, E.; Head-Gordon, M. Methane Storage: Molecular Mechanisms Underlying Room-Temperature Adsorption in Zn4O(BDC)3 (MOF-5). *J. Phys. Chem. C* **2017**, *121* (22), 12091–12100. https://doi.org/10.1021/acs.jpcc.7b04246.

(29) Yan, Y.; Kolokolov, D. I.; Da Silva, I.; Stepanov, A. G.; Blake, A. J.; Dailly, A.; Manuel, P.; Tang, C. C.; Yang, S.; Schröder, M. Porous Metal-Organic Polyhedral Frameworks with Optimal Molecular Dynamics and Pore Geometry for Methane Storage. *J. Am. Chem. Soc.* **2017**, *139* (38), 13349–13360. https://doi.org/10.1021/jacs.7b05453.

(30) Kim, A. R.; Yoon, T. U.; Kim, S. I.; Cho, K.; Han, S. S.; Bae, Y. S. Creating High CO/CO2 Selectivity and Large CO Working Capacity Through Facile Loading of Cu(I) Species into an Iron-Based Mesoporous Metal-Organic Framework. *Chem. Eng. J.* **2018**, *348* (April), 135–142. https://doi.org/10.1016/j.cej.2018.04.177.

(31) Kirchon, A.; Feng, L.; Drake, H. F.; Joseph, E. A.; Zhou, H.-C. From Fundamentals to Applications: A Toolbox for Robust and Multifunctional MOF Materials. *Chem. Soc. Rev.* **2018**, *47*, 8611–8638.

(32) Moghadam, P. Z.; Li, A.; Wiggin, S. B.; Tao, A.; Maloney, A. G. P.; Wood, P. A.; Ward, S. C.; Fairen-Jimenez, D. Development of a Cambridge Structural Database Subset: A Collection of Metal-Organic Frameworks for Past, Present, and Future. *Chem. Mater.* **2017**, *29* (7), 2618–2625. https://doi.org/10.1021/acs.chemmater.7b00441.

(33) Hönicke, I. M.; Senkovska, I.; Bon, V.; Baburin, I. A.; Bönisch, N.; Raschke, S.; Evans, J. D.; Kaskel, S. Balancing Mechanical Stability and Ultrahigh Porosity in Crystalline Framework Materials. *Angew. Chemie - Int. Ed.* **2018**, *57* (42), 13780–13783. https://doi.org/10.1002/anie.201808240.

(34) Peng, Y.; Krungleviciute, V.; Eryazici, I.; Hupp, J. T.; Farha, O. K.; Yildirim, T. Methane Storage in Metal − Organic Frameworks: Current Records, Surprise Findings, and Challenges. *J. Am. Chem. Soc* **2013**, *135*, 11887–11894. https://doi.org/10.1021/ja4045289.

(35) Kinoshita, Y.; Matsubara, I.; Higuchi, T.; Saito, Y. The Crystal Structure of Bis (Adiponitrilo) Copper (I) Nitrate. *Bull. Chem. Soc. Jpn.* **1959**, *32* (11), 1221–1226.

(36) Hoskins, B. F.; Robson, R. Design and Construction of a New Class of Scaffolding-like Materials Comprising Infinite Polymeric Frameworks of 3D-Linked Molecular Rods. A Reappraisal of the Zn(CN)2 and Cd(CN)2 Structures and the Synthesis and Structure of the Diamond-Related Framework. *J. Am. Chem. Soc.* **1990**, *112* (4), 1546–1554. https://doi.org/10.1021/ja00160a038.

(37) Aumüller, A.; Erk, P.; Klebe, G.; Hünig, S.; von Schütz, J. U.; Werner, H.-P. A Radical Anion Salt of 2,5-Dimethyl-N,N′-Dicyanoquinonediimine with Extremely High Electrical Conductivity. *Angew. Chemie Int. Ed. English* **1986**, *25* (8), 740–741.

https://doi.org/10.1002/anie.198607401.

(38) Li, H.; Eddaoudi, M.; Groy, T. L.; Yaghi, O. M. Establishing Microporosity in Open Metal-Organic Frameworks: Gas Sorption Isotherms for Zn(BDC) (BDC = 1,4-Benzenedicarboxylate). *J. Am. Chem. Soc.* **1998**, *120* (33), 8571–8572. https://doi.org/10.1021/ja981669x.

(39) Eddaoudi, M.; Li, H.; Yaghi, O. M. Highly Porous and Stable Metal-Organic Frameworks: Structure Design and Sorption Properties. *J. Am. Chem. Soc* **2000**, *122*, 1391–1397.

(40) Kondo, M.; Yoshitomi, T.; Seki, K.; Matsuzaka, H.; Kitagawa, S. Three-Dimensional Framework with Channeling Cavities for Small Molecules. *Angew. Chem. Int. Ed.* **1997**, *36* (16), 1725–1727. https://doi.org/1.

(41) Gómez-Gualdrón, D. A.; Wang, T. C.; García-Holley, P.; Sawelewa, R. M.; Argueta, E.; Snurr, R. Q.; Hupp, J. T.; Yildirim, T.; Farha, O. K. Understanding Volumetric and Gravimetric Hydrogen Adsorption Trade-Off in Metal-Organic Frameworks. *ACS Appl. Mater. Interfaces* **2017**, *9* (39), 33419–33428. https://doi.org/10.1021/acsami.7b01190.

(42) Colón, Y. J.; Fairen-Jimenez, D.; Wilmer, C. E.; Snurr, R. Q. High-Throughput Screening of Porous Crystalline Materials for Hydrogen Storage Capacity Near Room Temperature. *J. Phys. Chem. C* **2014**, *118* (10), 5383–5389. https://doi.org/10.1021/jp4122326.

(43) Tian, T.; Velazquez-Garcia, J.; Bennett, T. D.; Fairen-Jimenez, D. Mechanically and Chemically Robust ZIF-8 Monoliths With High Volumetric Adsorption Capacity. *J. Mater. Chem. A* **2015**, *3* (6), 2999–3005. https://doi.org/10.1039/C4TA05116E.

(44) Faust, T. MOFs Move to Market. *Nat. Chem.* **2016**, *8* (11), 990–991. https://doi.org/10.1038/nchem.2656.

(45) Valizadeh, B.; Nguyen, T. N.; Stylianou, K. C. Shape Engineering of Metal–Organic Frameworks. **2018**, *145*, 1–15.

(46) Thakkar, H.; Eastman, S.; Al-Naddaf, Q.; Rownaghi, A. A.; Rezaei, F. 3D-Printed Metal-Organic Framework Monoliths for Gas Adsorption Processes. *ACS Appl. Mater. Interfaces* **2017**, *9* (41), 35908–35916. https://doi.org/10.1021/acsami.7b11626.

(47) Kreider, M. C.; Sefa, M.; Fedchak, J. A.; Scherschligt, J.; Bible, M.; Natarajan, B.; Klimov, N. N.; Miller, A. E.; Ahmed, Z.; Hartings, M. R. Toward 3D Printed Hydrogen Storage Materials Made with ABS-MOF Composites. *Polym. Adv. Technol.* **2018**, *29* (2), 867–873. https://doi.org/10.1002/pat.4197.

(48) Chen, Y.; Huang, X.; Zhang, S.; Li, S.; Cao, S.; Pei, X.; Zhou, J.; Feng, X.; Wang, B. Shaping of Metal-Organic Frameworks: From Fluid to Shaped Bodies and Robust Foams. *J. Am. Chem. Soc.* **2016**, *138* (34), 10810–10813. https://doi.org/10.1021/jacs.6b06959.

(49) Stassen, I.; Styles, M.; Grenci, G.; Van Gorp, H.; Vanderlinden, W.; De Feyter, S.; Falcaro, P.; De Vos, D.; Vereecken, P.; Ameloot, R. Chemical Vapour Deposition of Zeolitic Imidazolate Framework Thin Films. *Nat. Mater.* **2016**, *15* (3), 304–310. https://doi.org/10.1038/nmat4509.

(50) Rezaei, F.; Lawson, S.; Hosseini, H.; Thakkar, H.; Hajari, A.; Monjezi, S.; Rownaghi, A. A. MOF-74 and UTSA-16 Film Growth on Monolithic Structures and Their CO2 Adsorption Performance. *Chem. Eng. J.* **2017**, *313*, 1346–1353. https://doi.org/10.1016/j.cej.2016.11.058.

(51) Lawson, S.; Hajari, A.; Rownaghi, A. A.; Rezaei, F. MOF Immobilization on the Surface of Polymer-Cordierite Composite Monoliths Through In-Situ Crystal Growth. *Sep. Purif. Technol.* **2017**, *183*, 173–180. https://doi.org/10.1016/j.seppur.2017.03.072.

(52) Fernández-Catalá, J.; Casco, M. E.; Martínez-Escandell, M.; Rodríguez-Reinoso, F.;

Silvestre-Albero, J. HKUST-1@ACM Hybrids for Adsorption Applications: A Systematic Study of the Synthesis Conditions. *Microporous Mesoporous Mater.* **2017**, *237*, 74–81. https://doi.org/10.1016/j.micromeso.2016.09.020.

(53) Nandasiri, M. I.; Jambovane, S. R.; McGrail, B. P.; Schaef, H. T.; Nune, S. K. Adsorption, Separation, and Catalytic Properties of Densified Metal-Organic Frameworks. *Coord. Chem. Rev.* **2016**, *311*, 38–52. https://doi.org/10.1016/j.ccr.2015.12.004.

(54) Dhainaut, J.; Avci-Camur, C.; Troyano, J.; Legrand, A.; Canivet, J.; Imaz, I.; Maspoch, D.; Reinsch, H.; Farrusseng, D. Systematic Study of the Impact of MOF Densification into Tablets on Textural and Mechanical Properties. *CrystEngComm* **2017**, *19* (29), 4211–4218. https://doi.org/10.1039/c7ce00338b.

(55) Su, Z.; Miao, Y. R.; Zhang, G.; Miller, J. T.; Suslick, K. S. Bond Breakage Under Pressure in a Metal-Organic Framework. *Chem. Sci.* **2017**, *8* (12), 8004–8011. https://doi.org/10.1039/c7sc03786d.

(56) Yuan, S.; Sun, X.; Pang, J.; Lollar, C.; Qin, J. S.; Perry, Z.; Joseph, E.; Wang, X.; Fang, Y.; Bosch, M.; et al. PCN-250 under Pressure: Sequential Phase Transformation and the Implications for MOF Densification. *Joule* **2017**, *1* (4), 806–815. https://doi.org/10.1016/j.joule.2017.09.001.

(57) Moghadam, P. Z.; Rogge, S. M. J.; Li, A.; Chow, C.-M.; Wieme, J.; Moharrami, N.; Aragones-Anglada, M.; Conduit, G.; Gomez-Gualdron, D. A.; Van Speybroeck, V.; et al. Structure-Mechanical Stability Relations of Metal-Organic Frameworks via Machine Learning. *Matter* **2019**, *1* (1), 219–234. https://doi.org/10.1016/j.matt.2019.03.002.

(58) Yang, Z.; Cao, L.; Li, J.; Lin, J.; Wang, J. Facile Synthesis of Cu-BDC/Poly(N-Methylol Acrylamide) HIPE Monoliths via CO2-in-Water Emulsion Stabilized by Metal-Organic Framework. *Polymer (Guildf).* **2018**, *153*, 17–23. https://doi.org/10.1016/j.polymer.2018.07.085.

(59) Yusuf, K.; Badjah-Hadj-Ahmed, A. Y.; Aqel, A.; Alothman, Z. A. Monolithic Metal-Organic Framework MIL-53(Al)-Polymethacrylate Composite Column for the Reversed-Phase Capillary Liquid Chromatography Separation of Small Aromatics. *J. Sep. Sci.* **2016**, *39* (5), 880–888. https://doi.org/10.1002/jssc.201501289.

(60) Zheng, J.; Cui, X.; Yang, Q.; Ren, Q.; Yang, Y.; Xing, H. Shaping of Ultrahigh-Loading MOF Pellet with a Strongly Anti-Tearing Binder for Gas Separation and Storage. *Chem. Eng. J.* **2018**, *354*, 1075–1082. https://doi.org/10.1016/j.cej.2018.08.119.

(61) Zhu, H.; Zhang, Q.; Zhu, S. Assembly of a Metal–Organic Framework into 3 D Hierarchical Porous Monoliths Using a Pickering High Internal Phase Emulsion Template. *Chem. Eur. J.* **2016**, *22* (26), 8751–8755. https://doi.org/10.1002/chem.201600313.

(62) Chanut, N.; Wiersum, A. D.; Lee, U. H.; Hwang, Y. K.; Ragon, F.; Chevreau, H.; Bourrelly, S.; Kuchta, B.; Chang, J. S.; Serre, C.; et al. Observing the Effects of Shaping on Gas Adsorption in Metal-Organic Frameworks. *Eur. J. Inorg. Chem.* **2016**, *2016* (27), 4416–4423. https://doi.org/10.1002/ejic.201600410.

(63) Finsy, V.; Ma, L.; Alaerts, L.; De Vos, D. E.; Baron, G. V.; Denayer, J. F. M. Separation of CO2/CH4 Mixtures With the MIL-53(Al) Metal-Organic Framework. *Micropor. Mesopor. Mat.* **2009**, *120* (3), 221–227. https://doi.org/10.1016/j.micromeso.2008.11.007.

(64) Valekar, A. H.; Lee, S. G.; Cho, K. H.; Lee, U. H.; Lee, J. S.; Yoon, J. W.; Hwang, Y. K.; Cho, S. J.; Chang, J. S. Shaping of Porous Metal-Organic Framework Granules Using Mesoporous ρ-Alumina as a Binder. *RSC Adv.* **2017**, *7* (88), 55767–55777. https://doi.org/10.1039/c7ra11764g.

(65) Rubio-Martinez, M.; Avci-Camur, C.; Thornton, A. W.; Imaz, I.; Maspoch, D.; Hill, M. R.

New Synthetic Routes Towards MOF Production at Scale. *Chem. Soc. Rev.* **2017**, *46* (11), 3453–3480. https://doi.org/10.1039/C7CS00109F.

(66) Tian, T.; Zeng, Z.; Vulpe, D.; Casco, M. E.; Divitini, G.; Midgley, P. A.; Silvestre-Albero, J.; Tan, J.-C.; Moghadam, P. Z.; Fairen-Jimenez, D. A Sol–Gel Monolithic Metal–Organic Framework with Enhanced Methane Uptake. *Nat. Mater.* **2018**, *17*, 174–179.

(67) Lim, G. J. H.; Wu, Y.; Shah, B. B.; Koh, J. J.; Liu, C. K.; Zhao, D.; Cheetham, A. K.; Wang, J.; Ding, J. 3D-Printing of Pure Metal–Organic Framework Monoliths. *ACS Mater. Lett.* **2019**, *1* (1), 147–153. https://doi.org/10.1021/acsmaterialslett.9b00069.

(68) Álvarez, J. R.; Sánchez-González, E.; Pérez, E.; Schneider-Revueltas, E.; Martínez, A.; Tejeda-Cruz, A.; Islas-Jácome, A.; González-Zamora, E.; Ibarra, I. A. Structure Stability of HKUST-1 Towards Water and Ethanol and Their Effect on Its CO2 Capture Properties. *Dalt. Trans.* **2017**, *46* (28), 9192–9200. https://doi.org/10.1039/C7DT01845B.

(69) Cavka, J. H.; Jokobsen, S.; Olsbye, U.; Guillou, N.; Lamberti, C.; Bordiga, S.; Lillerud, K. P. A New Zirconium Inorganic Building Brick Forming Metal Organic Frameworks with Exceptional Stability. *J. Am. Chem. Soc.* **2008**, *130*, 13850–13851. https://doi.org/10.1021/ja8057953.

(70) Bueken, B.; Van Velthoven, N.; Willhammar, T.; Stassin, T.; Stassen, I.; Keen, D. A.; Baron, G. V.; Denayer, J. F. M.; Ameloot, R.; Bals, S.; et al. Gel-Based Morphological Design of Zirconium Metal–Organic Frameworks. *Chem. Sci.* **2017**, *8* (5), 3939–3948.

(71) Solla, E. L.; Yot, P. G.; Horcajada, P. A Robust Monolithic Metal–Organic Framework with Hierarchical Porosity. *Chem. Commun.* **2018**, No. 54, 13088–13091.

(72) Hara, Y.; Kanamori, K.; Nakanishi, K. Self-Assembly of Metal-Organic Frameworks into Monolithic Materials with Highly Controlled Trimodal Pore Structures. *Angew. Chemie Int. Ed.* **2019**. https://doi.org/10.1002/anie.201911499.

(73) Connolly, B. M.; Mehta, J. P.; Moghadam, P. Z.; Wheatley, A. E. H.; Fairen-Jimenez, D. From Synthesis to Applications : Metal – Organic Frameworks for an Environmentally Sustainable Future. *Curr. Opin. Green Sustain. Chem.* **2018**, *12*, 47–56. https://doi.org/10.1016/j.cogsc.2018.06.012.

(74) Schoedel, A.; Ji, Z.; Yaghi, O. M. The Role of Metal–Organic Frameworks in a Carbon-Neutral Energy Cycle. *Nat. Energy* **2016**, *1* (4), 1–13.

(75) Alonso, A.; Moral-vico, J.; Abo, A.; Busquets-fité, M.; Komilis, D.; Puntes, V.; Sánchez, A.; Font, X. Critical Review of Existing Nanomaterial Adsorbents to Capture Carbon Dioxide and Methane. *Sci. Total Environ.* **2017**, *595*, 51–62. https://doi.org/10.1016/j.scitotenv.2017.03.229.

(76) Frameworks for Commercial Success. *Nat. Chem.* **2016**, *8* (11), 987. https://doi.org/10.1038/nchem.2661.

(77) DeSantis, D.; Mason, J. A.; James, B. D.; Houchins, C.; Long, J. R.; Veenstra, M. Techno-Economic Analysis of Metal–Organic Frameworks for Hydrogen and Natural Gas Storage. *Energy & Fuels* **2017**, *31* (2), 2024–2032. https://doi.org/10.1021/acs.energyfuels.6b02510.

(78) Howarth, A. J. Experimentalists and Theorists Need to Talk. *Nature* **2017**, *551* (7681), 433–434. https://doi.org/10.1038/d41586-017-07207-7.

(79) Guillerm, V.; Maspoch, D. Geometry Mismatch and Reticular Chemistry: Strategies to Assemble Metal-Organic Frameworks with Non-Default Topologies. *J. Am. Chem. Soc.* **2019**. https://doi.org/10.1021/jacs.9b08754.

(80) Coudert, F. X.; Fuchs, A. H. Computational Characterization and Prediction of Metal-Organic Framework Properties. *Coord. Chem. Rev.* **2016**, *307*, 211–236.

https://doi.org/10.1016/j.ccr.2015.08.001.

(81) Moghadam, P. Z.; Islamoglu, T.; Goswami, S.; Exley, J.; Fantham, M.; Kaminski, C. F.; Snurr, R. Q.; Farha, O. K.; Fairen-Jimenez, D. Computer-Aided Discovery of a Metal-Organic Framework with Superior Oxygen Uptake. *Nat. Commun.* **2018**, *9* (1), 1–8. https://doi.org/10.1038/s41467-018-03892-8.

(82) Petit, C. Present and Future of MOF Research in the Field of Adsorption and Molecular Separation. *Curr. Opin. Chem. Eng.* **2018**, *20*, 132–142. https://doi.org/10.1016/j.coche.2018.04.004.

TOC